Wedge-shaped subretinal hyporeflectivity in geographic atrophy

Querques, Giuseppe ; Capuano, Vittorio ; Frascio, Pietro ; Zweifel, Sandrine ; Georges, Anouk ; Souied, Eric H

DOI: https://doi.org/10.1097/IAE.0000000000000553

WEDGE-SHAPED SUBRETINAL HYPOREFLECTIVITY IN GEOGRAPHIC ATROPHY

GIUSEPPE QUERQUES, MD, PHD,*† VITTORIO CAPUANO, MD,* PIETRO FRASCIO, MD,* SANDRINE ZWEIFEL, MD,* ANOUK GEORGES, MD,* ERIC H. SOUIED, MD, PHD*

Purpose: To describe wedge-shaped subretinal hyporeflectivity, a peculiar spectral domain optical coherence tomography finding in geographic atrophy (GA) areas of atrophic age-related macular degeneration.

Methods: We reviewed the charts of consecutive patients with GA who presented between January 2012 and December 2013. A standardized imaging protocol was performed in all patients, which included blue fundus autofluorescence, and spectral domain optical coherence tomography.

Results: Wedge-shaped subretinal hyporeflective lesions were found in 12 of 161 included eyes (11 of 94 consecutive patients, 6 males/5 females, mean age 79.6 ± 9.3 years). On spectral domain optical coherence tomography, regions immediately adjacent to the wedge-shaped subretinal hyporeflective lesions were characterized by absence of the hyporeflective outer nuclear layer, the hyperreflective external limiting membrane, the ellipsoid zone, the interdigitation zone, and the retinal pigment epithelium. On "en face" images, they appeared as round-oval hyporeflectivities delimited by hyperreflective borders, which we interpreted as the outer plexiform layer. Mean GA area was significantly larger in eyes with as compared with eyes without wedge-shaped subretinal hyporeflective lesions. Overall, the dimensions of the wedge-shaped subretinal hyporeflective lesions did not change after a mean of ~15 months.

Conclusion: Wedge-shaped subretinal hyporeflectivity, a previously unreported peculiar finding in GA areas of atrophic age-related macular degeneration eyes, appears delimited internally by the hyperreflective outer plexiform layer and externally by the hyperreflective Bruch membrane. These lesions, which are detected in eyes with large GA (even though stable over time), should be recognized and distinguished from subretinal fluid (and other exudative signs of age-related macular degeneration) because their presence should not require prompt treatment.

RETINA 35:1735–1742, 2015

Age-related macular degeneration (AMD), the most common cause of legal blindness among elderly individuals in developed countries, may have two different phenotypes, the neovascular and the atrophic.[1,2] Geographic atrophy (GA) represents the atrophic late-stage manifestation of AMD and is responsible for approximately 35% of all cases with late AMD.[3,4] It is defined as a sharply demarcated, large (generally >200 μm), round/oval, confluent area of hypopigmentation with loss of retinal pigment epithelium (RPE) and outer neurosensory retina.[5,6] Geographic atrophy is characterized by a dense scotoma, which generally corresponds in spatial extent exactly to the atrophic area (where the photoreceptor layer and the RPE deteriorate and finally necrose).[7]

Studies have shown that the primary cells affected by GA are those in the RPE; RPE atrophy is followed by photoreceptor apoptosis and choriocapillaris atrophy.[8–10] Currently, several trials are investigating treatments that may slow down GA progression. However, there is as yet no treatment available for patients

From the *Department of Ophthalmology, Centre Hospitalier Intercommunal de Creteil, University Paris Est Creteil, Creteil, France; and †Department of Ophthalmology, University Scientific Institute San Raffaele, Milan, Italy.

None of the authors have any financial/conflicting interests to disclose.

Reprint requests: Giuseppe Querques, MD, PhD, Department of Ophthalmology, Centre Hospitalier Intercommunal de Creteil, University Paris Est Creteil, 40 Avenue de Verdun, 94000 Creteil, France; e-mail: giuseppe.querques@hotmail.it

with GA. A better understanding of the physiopathologic features of GA is required to identify potential targets for intervention.

Recent developments in imaging technologies have enabled the noninvasive in vivo study of different retinal disorders, including GA, with unprecedented resolution, and thus provided further insights in the diseases process.[11–17] Using spectral domain optical coherence tomography (SD-OCT), a recently introduced technology with improved resolution and speed compared with previous time-domain OCT, we observed a peculiar finding in some GA areas of atrophic AMD eyes, a wedge-shaped subretinal hyporeflectivity. The purpose of this study was to describe and interpret this peculiar SD-OCT finding in GA eyes.

Methods

We reviewed the charts of all consecutive patients with GA due to AMD that presented at the University Eye Clinic of Creteil between January 2012 and December 2013. Criteria for inclusion were age >50 years, diagnosis of AMD, and presence of GA defined as any sharply demarcated unifocal or multifocal area of apparent absence of the RPE, larger than 750 μm (diameter), with visible choroidal vessels with no signs of choroidal neovascularization (CNV), intraretinal or subretinal fluid, or hemorrhage. Exclusion criteria were significant media opacities, evidence of diabetic retinopathy or any other retinal vascular disease, CNV, subretinal fibrosis, vitreoretinal disease, myopia >6 D, any previous treatment (e.g., laser photocoagulation, photodynamic therapy, intravitreal injections of steroids, or antivascular endothelial growth factor), and signs or history of hereditary retinal dystrophy.

All patients underwent best-corrected visual acuity using standard Early Treatment Diabetic Retinopathy Study charts, slit-lamp examination, fundus biomicroscopy, blue fundus autofluorescence (FAF), and SD-OCT. This study was conducted in accordance with French bioethical legislation and the Declaration of Helsinki for research involving human subjects. French Society of Ophthalmology Institutional Review Board approval was obtained for this study.

Simultaneous recordings of SD-OCT and confocal scanning ophthalmoscope infrared or FAF images were obtained with a combined imaging system (Spectralis HRA + OCT; Heidelberg Engineering, Heidelberg, Germany). A standardized imaging protocol was performed in all patients, which included acquisition of infrared reflectance (820 nm; field of view, 30° × 30°; image resolution 768 × 768 pixels) or blue FAF (excitation λ = 488 nm; emission λ > 500 nm; field of view, 30° × 30°; image resolution 768 × 768 pixels), and simultaneous SD-OCT scanning using a second, independent pair of scanning mirrors (λ = 870 nm; acquisition speed, 40,000 A-scans per seconds; scan depth, 1.8 mm; digital depth resolution, approximately 3.5 μm per pixel; optical depth resolution, 7 μm; lateral optical resolution, 14 μm). With confocal image acquisition, light from a conjugate plane of interest is detected by the image sensor, permitting suppression of light from planes anterior and posterior to the plane of interest and resulting in high-contrast fundus images. Using automated eye tracking and image alignment based on confocal scanning ophthalmoscope images, the software allows averaging a variable number of single images in real time (Automatic Real Time Module; Heidelberg Engineering).

The SD-OCT minimum acquisition protocol included 19 horizontal lines, each composed of 9 averaged OCT B-scans (1,024 A scans per line) at 240-μm intervals, covering a 6- × 6-mm area; further high-resolution 9-mm single B-scans (each composed of up to 100 averaged enhanced depth imaging OCT B-scans)[11] were guided from GA areas. In a subset of eyes, 97 sections, each comprised 9 averaged enhanced depth imaging OCT B-scans at 30-μm intervals, were obtained within a 15° × 10° rectangle to encompass the GA area. The SD-OCT images (single B-scans and the 496 "en face" images, from the vitreous cavity and inner retinal surface up to the outer sclera) consecutively collected were viewed with the contained Heidelberg Eye Explorer software (version 1.7.0.0; Heidelberg Engineering).

Qualitative descriptions were independently performed by 2 senior retinal physicians (G.Q. and E.H.S.) on the high-quality confidently tracked (FAF and infrared images) SD-OCT scans. Disagreement between readers regarding the detection of features was resolved by open adjudication. To describe the SD-OCT images, according to Spaide and Curcio,[12] the following correspondence has been applied to the outer retinal layers (Figure 1): The innermost highly reflective band reflects the external limiting membrane (ELM); a second band corresponds to the photoreceptors' inner segment ellipsoid portion/outer segment interface, also known as the "ellipsoid zone"[13]; a third band represents the RPE/outer segment junction, also known as "interdigitation zone"[13]; and the most external band corresponds to the RPE/Bruch membrane (BM) complex. The hyperreflective layer and the 2 hyporeflective layers internal to the ELM correspond to the outer plexiform layer (OPL) and to the inner nuclear layer and the outer nuclear layer (ONL), respectively (Figure 1).[14–16]

The greatest linear dimensions for both the horizontal and vertical planes and the wedge-shaped

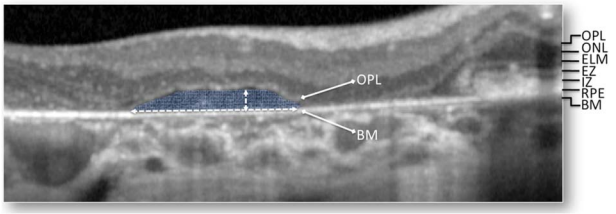

Fig. 1. Enlarged SD-OCT view of a wedge-shaped subretinal hyporeflective lesion showing how the greatest linear dimensions for both the horizontal and vertical planes and the lesion area were measured manually using the Heidelberg Eye Explorer software (version 1.7.0.0; Heidelberg Engineering). The innermost band reflects the ELM; the second band corresponds to the photoreceptors' inner segment ellipsoid portion/outer segment (OS) interface, also known as the "ellipsoid zone" (EZ); the third band represents the RPE/OS junction, also known as "interdigitation zone" (IZ); the most external band corresponds to the RPE/BM complex. The hyporeflective layer and hyperreflective layer internal to the ELM correspond the ONL and the OPL, respectively.

subretinal hyporeflective lesion area were measured manually by 2 senior retinal physicians (G.Q. and E.H. S.) on the Heidelberg Eye Explorer software (version 1.7.0.0; Heidelberg Engineering) as displayed in Figure 1 (mean values were used for calculations). Pixel values were calculated in micrometers by using the scale factor given by the software. This factor is based on a Gullstrand eye, assuming standard corneal radii and taking into account the individual spherical refraction as adjusted by the operator during acquisition.

When available, repeated SD-OCT examinations (matching the GA areas characterized by the presence of wedge-shaped subretinal hyporeflective lesions) were also investigated about changes over time. Spectralis SD-OCT allows confidently detecting and assessing small changes over time by using confocal scanning ophthalmoscope technology to track the eye and guide OCT to the selected location. By using a selected previous reference scan, the Spectralis SD-OCT aligns the reference fundus image with the live patient fundus image at follow-up. The eye tracker recognizes the retina and then directs the SD-OCT scan to the same location. This eliminates the potential bias of subjective placement of the scan by the operator.

For each study eye, identification and quantification of atrophy was performed on FAF images using Region Finder (Region Finder, version 2.4.3; Heidelberg Engineering). Region Finder is a software embedded in Spectralis (Spectralis HRA + OCT; Heidelberg Engineering) that performs semiautomated identification and quantification of atrophic areas allowing FAF images to be directly processed. This software has been described and validated in a recent study.[17] For each FAF frame, pixel intensity quantification is done in a gray scale. The operator must define the center of the region, which he determines to be an atrophic area, and then the software algorithm expands this zone after decreasing of gray scale levels that resemble those initially chosen, allowing, thus, for a very precise measure of atrophic areas. In the current analysis, digital images had a resolution of 768 × 768 pixels (30° × 30° frame), and thus each pixel corresponded to 11 μm^2. When available, repeated FAF examinations were also investigated using Region Finder about changes of GA progression over time.

The statistical analysis included descriptive statistics for demographic data (Fisher's exact test), an estimation of the prevalence of the wedge-shaped subretinal hyporeflective lesions in atrophic areas among patients with GA with 95% confidence intervals, qualitative descriptions of the findings, and quantitative analyses and comparisons during the study period (from study entry to last follow-up visit; Student's *t*-test and Wilcoxon test). Cohen's kappa coefficient was performed to measure the agreement between readers regarding the manual measurements of wedge-shaped subretinal hyporeflective lesion greatest linear dimensions and areas. Data were analyzed with the Statistical Package for the Social Sciences version 20.0 for Mac (IBM, Chicago, IL).

Results

Ninety-four consecutive patients (70 females and 24 males; mean age 79.7 ± 9.0 years) were included in the retrospective analysis. Sixty-seven patients had GA in both eyes. Twenty-seven fellow eyes were excluded because of absence of GA (11 eyes), subretinal fibrosis (8 eyes), and previous treatment for CNV (intravitreal injections of antivascular endothelial growth factor in 8 eyes).

Of the 161 eyes retrospectively investigated about the presence of wedge-shaped subretinal hyporeflectivities in GA areas, 12 eyes of 11 patients showed the peculiar finding on SD-OCT (Table 1). This accounts for an estimated prevalence of wedge-shaped subretinal hyporeflective lesions in atrophic areas among patients with GA of 11.7% (95% confidence interval, 0.06–0.19). It is noteworthy that the bilateral lesions were less common in bilateral GA patients (estimated prevalence in 95% confidence interval, −0.04 to 0.12) as only 1 patient showed wedge-shaped subretinal hyporeflectivies in both eyes (1% of bilateral wedge-shaped subretinal hyporeflective lesions in bilateral GA vs. 14% of unilateral wedge-shaped subretinal hyporeflective lesions in bilateral GA; $P = 0.01$ through Fisher's exact test). Mean best-corrected visual acuity and GA areas measurements at inclusion and their changes during the study period are reported in Table 1.

A total of 15 wedge-shaped subretinal hyporeflective lesions were detected in GA areas by our minimum

Table 1. Demographics and Clinical Features of Patients With GA, With and Without Wedge-Shaped Subretinal Hyporeflectivity

	With Wedge-Shaped Subretinal Hyporeflectivity	Without Wedge-Shaped Subretinal Hyporeflectivity	*P*
Gender, n			
Male	6	18	
Female	5	65	0.02*
Age (mean ± SD), years	79.6 ± 9.3	81.3 ± 5.3	0.21†
Study period (mean ± SD), months	15.0 ± 5.4	15.7 ± 5.07	0.73†
logMAR, mean ± SD			
First visit	0.8 ± 0.4	0.9 ± 0.5	0.65‡
Last visit	0.9 ± 0.4	0.9 ± 0.5	0.83‡
Atrophic area§ (median), mm^2			
First visit	11.8 ± 5.9 (10.7)	6.5 ± 4.9 (7.1)	0.008† 0.006‡
Last visit	13.1 ± 7.0 (12.3)	9.76 ± 7.3 (8.6)	0.25† 0.25‡
∂	2.1 ± 1.2 (1.6)	3.2 ± 3.6 (1.6)	0.39† 0.91‡
ORT, n of eyes (%)	2 (16.6)	26 (16.1)	0.96‡

*Fisher's exact test.
†Student's *t*-test.
‡Wilcoxon test.
§Quantitative analysis by Region Finder, ∂ (delta): difference on size of atrophic area.

SD-OCT acquisition protocol (mean 1.3 lesions per eye). Two lesions were located in the fovea, whereas among the 13 extrafoveal lesions, 4 were located superiorly, 3 inferiorly, 3 nasally, and 3 temporally.

On SD-OCT B-scan, regions immediately adjacent to the wedge-shaped subretinal hyporeflective lesions were characterized by an absence of the hyporeflective ONL, the hyperreflective ELM, the ellipsoid zone, the interdigitation zone, and the RPE (Figure 1). The thin remainder of the outermost hyperreflective layer was interpreted as the BM (Figure 1).[16] In these regions, the OPL approaches the BM (Figure 1).[16] By assuming such changes in the outer retinal layers of adjacent regions, the wedge-shaped subretinal hyporeflective lesions appeared on SD-OCT B-scan delimited internally by the hyperreflective OPL and externally by the hyperreflective BM (Figure 1). On "en face" images, they appeared as round-oval hyporeflectivities delimited by hyperreflective borders (i.e., the OPL) (Figure 2). It is noteworthy that, despite being mostly hyporeflective, some variable reflective punctate material was observed in these subretinal lesions (Figures 2 and 3). Interestingly, the lesions showed slight autofluorescence within an area of hypo-FAF due to GA (Figures 2 and 3).

When the wedge-shaped subretinal hyporeflective lesions were found adjacent to outer retinal tubulations (ORTs),[18] both appeared delimited externally by the hyperreflective BM. However, no hyperreflective OPL was detected internal to the ORTs (Figure 4). The prevalence of ORTs was similar in both the group with and without the wedge-shaped lesions (Table 1).

The greatest linear dimensions for both the horizontal and vertical planes, and the wedge-shaped subretinal hyporeflective lesions area at inclusion, and their changes during the study period (7 eyes), are reported in Table 2 (Figure 5).

Discussion

In this study, we report wedge-shaped subretinal hyporeflectivity as a peculiar SD-OCT finding in GA areas of atrophic AMD eyes. The retina overlying each of these hyporeflective lesions was characterized on SD-OCT B-scan by an absence of the hyporeflective ONL, the hyperreflective ELM, the ellipsoid zone, the interdigitation zone, and the RPE (Figure 1); thus, the wedge-shaped lesions appeared delimited internally by the hyperreflective OPL and externally by the hyperreflective BM (Figure 1). On "en face" SD-OCT, the lesions appeared as round-oval hyporeflectivities delimited by hyperreflective borders (i.e., the OPL) (Figure 2).

It is noteworthy that the wedge-shaped subretinal hyporeflective lesions were combined with variable reflective punctate material (Figures 2 and 3), which may be responsible for the corresponding slight autofluorescent signal recorded on blue FAF (Figures 2 and 3). This suggests the presence of fluorophore-enriched debris (i.e., outer segment material that has not been phagocytosed) in the composition of wedge-shaped subretinal hyporeflective lesions.[5,15] Sarks et al[5] reported that in GA areas, the ONL disappears

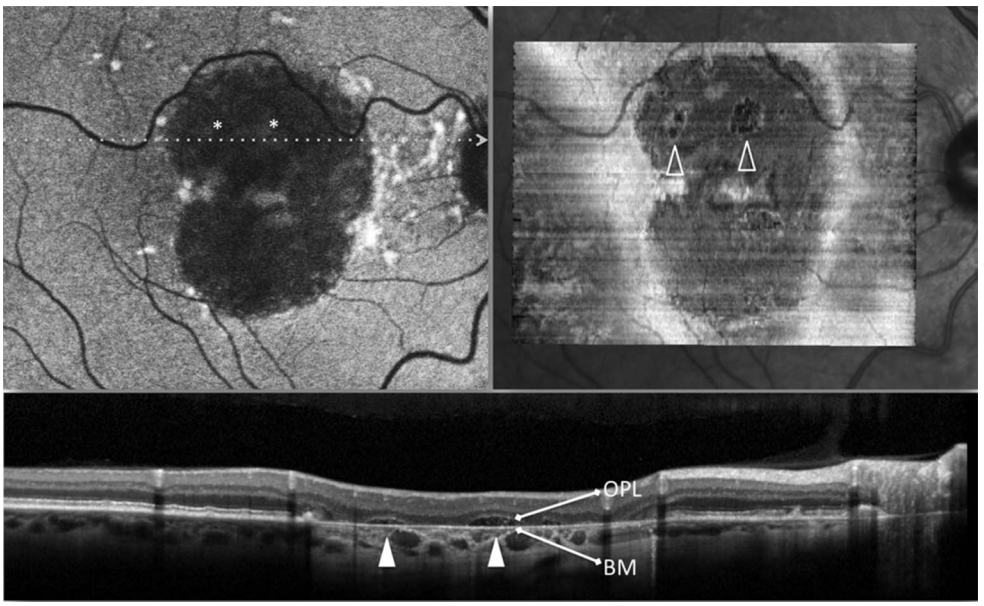

Fig. 2. Spectral domain optical coherence tomography (B-scan and "en face" images) and FAF of wedge-shaped subretinal hyporeflective lesions. On SD-OCT B-scan, the wedge-shaped subretinal hyporeflective lesions appear delimited internally by the hyperreflective OPL and externally by the hyperreflective BM (arrowheads). On "en face" image, they appeared as round-oval hyporeflectivities delimited by hyperreflective borders (the OPL) (open arrowheads). The lesions show slight autofluorescence within an area of hypo-FAF due to geographic atrophy (asterisks).

and, since the RPE and the ELM also disappeared, an attenuated OPL rests directly on the basal laminar deposits. Therefore basal laminar deposits and other residual sub-RPE deposits[15] may also participate in the composition of wedge-shaped subretinal hyporeflective lesions.

Wedge-shaped subretinal hyporeflective lesions should be recognized and distinguished from subretinal

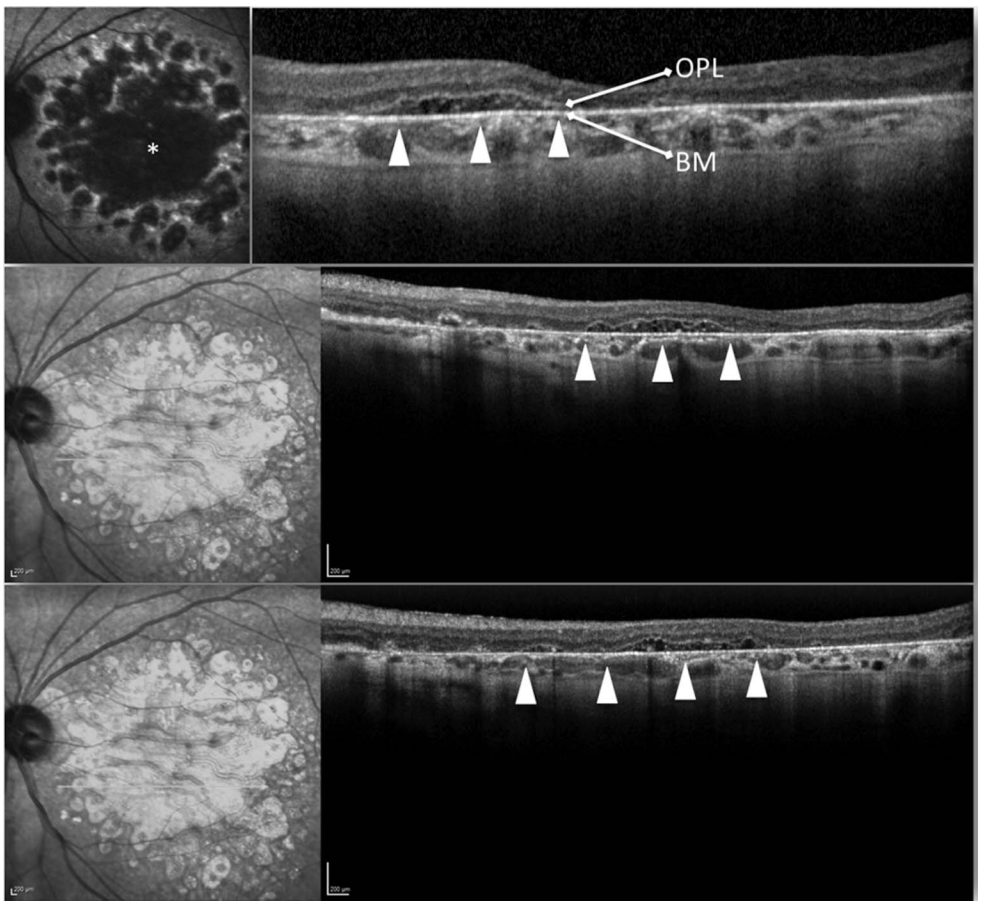

Fig. 3. Spectral domain optical coherence tomography and FAF of wedge-shaped subretinal hyporeflective lesions. On SD-OCT B-scans (three sequential scans, from the fovea to the inferior macula), the wedge-shaped subretinal hyporeflective lesions appear delimited internally by the hyperreflective OPL and externally by the hyperreflective BM (arrowheads). The lesions show slight autofluorescence within an area of hypo-FAF due to geographic atrophy (asterisk).

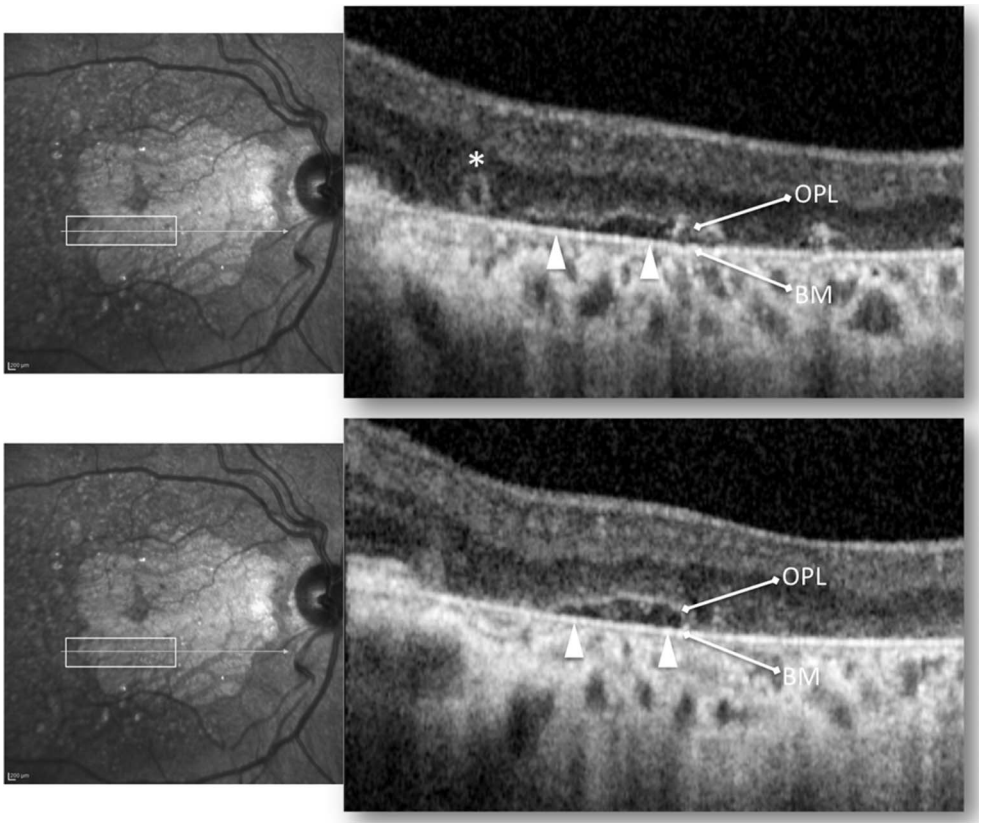

Fig. 4. Spectral domain optical coherence tomography of wedge-shaped subretinal hyporeflective lesions. On SD-OCT B-scans (two sequential scans, in the inferior macula), the wedge-shaped subretinal hyporeflective lesions appear delimited internally by the hyperreflective OPL and externally by the hyperreflective BM (arrowheads). Note, when the wedge-shaped subretinal hyporeflective lesion is adjacent to an ORT (asterisk), both appear delimited externally by the hyperreflective BM, and no hyperreflective OPL is detected internal to the ORT.

fluid, which can be a sign of CNV, because their presence should not require prompt treatment. In the current series, in any case, there was no evidence of CNV. Differently from subretinal fluid secondary to CNV, wedge-shaped subretinal hyporeflective lesions appeared delimited internally by the OPL, and despite being mostly hyporeflective, some variable reflective punctate material was observed within the lesions.

Recently, Cohen et al[19] reported on a relatively frequent retinal finding of atrophic AMD that they called retinal pseudocysts. Similarly to wedge-shaped subretinal hyporeflective lesions, eyes with retinal pseudocystic lesions showed no evidence of CNV. The authors proposed that retinal pseudocysts may correspond to Müller cell degeneration, and not to exudation, and thus, as for wedge-shaped subretinal hyporeflective lesions, their presence should not require prompt treatment.

Zweifel et al[18] recently described ORTs as branching tubular structures located in the ONL in a variety of advanced degenerative retinal disorders, including GA. Outer retinal tubulations appear as round or ovoid hyporeflective spaces with hyperreflective borders on OCT sections, and, similarly to wedge-shaped subretinal hyporeflective lesions, should be distinguished from exudative intraretinal and subretinal fluid because their presence do not require prompt treatment. The authors hypothesized that in eyes with atrophic disorders, the degenerating photoreceptors become arranged in a tubular fashion.[18] As for wedge-shaped subretinal hyporeflective lesions, also ORTs in atrophic areas contain hyperautofluorescent material.[18] This suggests the presence of degenerating photoreceptor or other fluorophore-enriched debris in the composition of both lesions. It is noteworthy that, in the current series, when ORTs were found adjacent to the wedge-shaped subretinal hyporeflective lesions, they appeared often delimited externally by the hyperreflective BM, but no hyperreflective OPL was detected internal to the ORT (Figure 4); however, the inner nuclear layer seemed not affected (as described by Sarks et al[5] in the evolution of GA).

Fleckenstein et al[15] using SD-OCT described in GA areas elevations with crownlike appearance with presumed debris beneath. Recently, Bonnet et al[20] reported on hyperreflective structures in GA areas, which the authors suggested to name as "ghost drusen." As for wedge-shaped subretinal hyporeflective lesions, also these structures, which were smaller and crownlike/pyramidal rather than wedge-shaped, often correlated with an increased FAF signal within the atrophy.

Table 2. Wedge-Shaped Subretinal Hyporeflective Lesions Characteristics, and Their Changes During the Study Period in 7 Eyes

	First Visit	Last Visit	*P*
Greatest linear dimension—horizontal, mean ± SD, μm	613.86 ± 322.26 (0.78†)	515.88 ± 236.88 (0.87†)	0.43*
Greatest linear dimension—vertical, μm	63.26 ± 26.60 (0.85†)	54.55 ± 18.29 (0.87†)	0.39*
Area, mean ± SD, mm^2	0.029 ± 0.02 (0.83†)	0.020 ± 0.01 (0.83†)	0.27*

*Student's *t*-test.
†Cohen's K coefficient.

Recognition of wedge-shaped subretinal hyporeflective lesions may be of great importance because several clinical studies, which are currently testing potential therapies for atrophic AMD, are using SD-OCT to monitor the disease progression. Natural history of atrophic AMD may possibly differ in presence/absence of wedge-shaped subretinal hyporeflective lesions; moreover, new upcoming treatments may differently affect the prognosis in presence/absence of these lesions.

While in the current series, there was no difference in age and best-corrected visual acuity, and females were significantly more numerous in the group of GA patients without as compared with patients with wedge-shaped subretinal hyporeflective lesions (Table 1). Interestingly, mean GA area as evaluated by semiautomated Region Finder software was significantly larger in eyes with as compared with eyes without wedge-shaped subretinal hyporeflective lesions (Table 1). Of note, this difference was no more significant after a mean of ~15 months (Table 1). Moreover, the greatest linear dimensions for both the horizontal and vertical planes and the wedge-shaped subretinal hyporeflective lesion area did not change after a mean of ~15 months (even though we recorded a trend to smaller dimensions/area at the last visit) (Table 2). Taken together, these findings suggest the presence of wedge-shaped subretinal hyporeflective lesions to be associated with a more advanced, even though stable, form of GA.

Our study has several limitations attributable mainly to its retrospective design and to the few included eyes. This retrospective analysis did not allow us to understand why wedge-shaped subretinal hyporeflective lesions developed only in a minority of GA eyes. Future studies will investigate the lesions predisposing to wedge-shaped subretinal hyporeflectivity development.

In conclusion, using SD-OCT, we described wedge-shaped subretinal hyporeflectivity, a previously

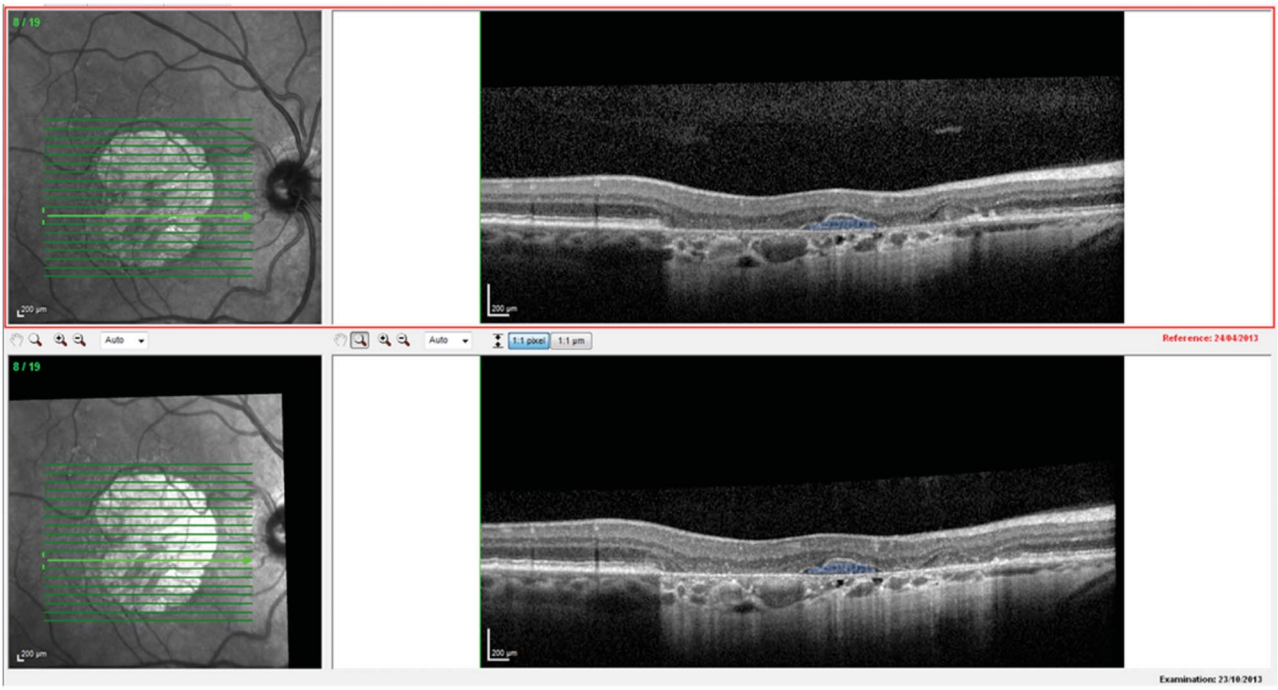

Fig. 5. Repeated SD-OCT of wedge-shaped subretinal hyporeflective lesions. Spectral domain optical coherence tomography examinations matching the geographic atrophy area characterized by the presence of wedge-shaped subretinal hyporeflectivities show no changes in the lesions area over 6 months.

unreported peculiar finding in some GA areas of atrophic AMD eyes. Wedge-shaped subretinal hyporeflective lesions appear delimited internally by the hyperreflective OPL and externally by the hyperreflective BM. These lesions, which are detected in eyes with large GA (even though stable over time), should be recognized and distinguished from subretinal fluid (and other exudative signs of CNV) because their presence should not require prompt treatment.

Key words: autofluorescence, age-related macular degeneration, atrophy, geographic atrophy, spectral domain optical coherence tomography.

References

1. Resnikoff S, Pascolini D, Etya'ale D, et al. Global data on visual impairment in the year 2002. Bull World Health Organ 2004;82:844–851.
2. Bressler NM, Bressler SB, Fine SL. Age-related macular degeneration. Surv Ophthalmol 1988;32:375–413.
3. Klein R, Klein BE, Knudtson MD, et al. Fifteen-year cumulative incidence of age-related macular degeneration: the Beaver Dam Eye Study. Ophthalmology 2007;114:253–262.
4. Augood CA, Vingerling JR, de Jong PT, et al. Prevalence of age related maculopathy in older Europeans: the European Eye Study (EUREYE). Arch Ophthalmol 2006;124:529–535.
5. Sarks JP, Sarks SH, Killingsworth MC. Evolution of geographic atrophy of the retinal pigment epithelium. Eye 1988;2:552–577.
6. Sunness JS, Bressler NM, Maguire MG. Scanning laser ophthalmoscopic analysis of the pattern of visual loss in age-related geographic atrophy of the macula. Am J Ophthalmol 1995;119:143–151.
7. Blair CJ. Geographic atrophy of the retinal pigment epithelium. A manifestation of senile macular degeneration. Arch Ophthalmol 1975;93:19–25.
8. Curcio CA, Medeiros NE, Millican CL. Photoreceptor loss in age-related macular degeneration. Invest Ophthalmol Vis Sci 1996;37:1236–1249.
9. Dunaief JL, Dentchev T, Ying GS, Milam AH. The role of apoptosis in age-related macular degeneration. Arch Ophthalmol 2002;120:1435–1442.
10. Hageman GS, Luthert PJ, Victor Chong NH, et al. An integrated hypothesis that considers drusen as biomarkers of immune-mediated processes at the RPE-Bruch's membrane interface in aging and age-related macular degeneration. Prog Retin Eye Res 2001;20:705–732.
11. Spaide RF, Koizumi H, Pozonni MC. Enhanced depth imaging spectral-domain optical coherence tomography. Am J Ophthalmol 2008;146:496–500.
12. Spaide RF, Curcio CA. Anatomical correlates to the bands seen in the outer retina by optical coherence tomography: literature review and model. Retina 2011;31:1609–1619.
13. Spaide RF. Questioning optical coherence tomography. Ophthalmology 2012;119:2203–2204. e1.
14. Pircher M, Gotzinger E, Findl O, et al. Human macula investigated in vivo with polarization-sensitive optical coherence tomography. Invest Ophthalmol Vis Sci 2006;47:5487–5494.
15. Fleckenstein M, Charbel Issa P, Helb HM, et al. High-resolution spectral domain-OCT imaging in geographic atrophy associated with age-related macular degeneration. Invest Ophthalmol Vis Sci 2008;49:4137–4144.
16. Fleckenstein M, Schmitz-Valckenberg S, Adrion C, et al. Tracking progression with spectral-domain optical coherence tomography in geographic atrophy caused by age-related macular degeneration. Invest Ophthalmol Vis Sci 2010;51:3846–3852.
17. Schmitz-Valckenberg S, Brinkmann CK, Alten F, et al. Semiautomated image processing method for identification and quantification of geographic atrophy in age-related macular degeneration. Invest Ophthalmol Vis Sci 2011;52:7640–7646.
18. Zweifel SA, Engelbert M, Laud K, et al. Outer retinal tubulation: a novel optical coherence tomography finding. Arch Ophthalmol 2009;127:1596–1602.
19. Cohen SY, Dubois L, Nghiem-Buffet S, et al. Retinal pseudocysts in age-related geographic atrophy. Am J Ophthalmol 2010;150:211–217.
20. Bonnet C, Querques G, Zerbib J, et al. Hyperreflective pyramidal structures on optical coherence tomography in geographic atrophy areas. Retina 2014;34:1524–1530.